Received: 8 September 2020 | Revised: 11 November 2020 | Accepted: 13 November 2020

DOI: 10.1002/pat.5183

RESEARCH ARTICLE

polymers advanced technologies WILEY

Calcium phosphate nanocomposites via in situ mineralization in block copolymer hydrogels

David M. Griffin[1,2] | Mitchell A. Kennedy[3] | Surita R. Bhatia[3]

[1]Department of Chemical Engineering, University of Massachusetts Amherst, Amherst, Massachusetts

[2]Department of Chemical and Petroleum Engineering, University of Kansas, Lawrence, Kansas

[3]Department of Chemistry, Stony Brook University, Stony Brook, New York

Correspondence
Surita R. Bhatia, Department of Chemistry, Stony Brook University, Stony Brook, NY 11794-3400.
Email: surita.bhatia@stonybrook.edu

Funding information
National Institutes of Health, Grant/Award Number: T32 GM08515; National Science Foundation, Grant/Award Numbers: 0504485, 0531171, 0654128, 1922639

Significant research has been directed toward producing composites that mimic the micro- to nanoscale structure of bone tissue, and it remains a challenge to develop synthetic strategies to create cost-effective biocomposite materials with nanoscale inorganic domains. In this paper, we report the synthesis of nanocrystalline calcium phosphate minerals in situ in gels of a commercially available block copolymer, Pluronic F127 (F127). Although solutions of F127 have previously been explored as a templating agent for calcium phosphate mineralization, here we demonstrate the synthesis of nano-sized calcium hydrogen phosphate hydrate directly in F127 gels. Composites formed at pH 7 contained highly crystalline, millimeter-scale crystals of brushite, while composites created at an initial pH of 11 contained nanoscale particles of a calcium hydrogen phosphate hydrate similar to natural bone apatite in morphology and size, with a mean particle diameter of 120 nm. The in situ composites have storage moduli of 15–25 kPa, which is comparable to mechanically processed hydrogel composites containing four times more inorganic material. We believe that our synthetic strategy may provide a new class of versatile and cost-effective nanostructured biomaterials for use in understanding and replicating mineralized tissues.

KEYWORDS
biomaterial, calcium phosphate, hydrogel, nanocomposite, Pluronics

1 | INTRODUCTION

Bone tissue is a complex biocomposite with organization on multiple length scales. Up to 90% of human bone is composed of hydrated Type I collagen fibrils mineralized with a carbonated apatite (dahllite). Collagen is composed of densely packed fibrils, each of which is composed of three individual strands in a triple helix. The fibrils are staggered in to form channels and can form complex 3D architectures.[1] Within the collagen fibrils, nanometer-scale plate-like crystals of bone apatite are found in a highly oriented configuration with the crystallographic *c*-axis lying parallel to the long axis of the protein molecule.[2] The mechanism of bone formation is still not precisely defined; although acidic amino acids of collagen, specifically aspartic acid and glutamic acid, are believed to initiate apatite nucleation. While collagen alone can induce the formation and direction of apatite crystallization, noncollagenous proteins and lipids present in the bone tissue likely also have roles such as calcium localization and crystal stabilization.[1,3]

One of the most common methods of treating serious fractures and chronic bone damage is by bone grafts, but there are limitations in the amount of donated tissue and donor and graft site morbidities.[4] Because of this, synthetic hydroxyapatite (HAp; $Ca_{10}(PO_4)_6(OH)_2$) has received a great deal of attention for uses in bone defect and articular cartilage repair due to its chemical and structural similarity to bone apatite.[5,6] Polymer composites containing hydroxyapatite have become desirable in biomaterial design due largely to tunable mechanical properties and improved biocompatibility.[7,8] Previous work has concluded that cell growth rate and viability show a dependence on the mechanical properties of the cells' local environment.[9] To properly integrate with and support encapsulated and surrounding cells, biomaterials must possess moduli similar to the tissue in which they are implanted. Polymeric composite biomaterials are ideal for these

applications as their material strength can be tuned by varying the ratio of polymer to inorganic (mineral) component.

An additional feature of hydroxyapatite, which makes it an ideal inorganic component for composite biomaterials, is its bioresorbable nature. When combined with a biodegradable or bioresorbable polymer component, composites containing hydroxyapatite can be naturally broken down in vivo. Bioresorbability of calcium phosphates is dependent not only on the mineral phase but also the degree of crystallinity and crystallite size. Nanoscopic, poorly crystalline calcium phosphates tend to show a higher propensity for resorption, on the level of biological apatite, whereas traditional microscopic crystals show poor solubility.[10] This characteristic motivates the need for a complete understanding of the phase, size, and morphology of composites' inorganic component.

Crystallite size of the ceramic used has also been shown to play an important role in the effectiveness of biomaterials used for growing osteoblasts (bone cells). Osteoblasts grown in vitro on nanoscale ceramic materials showed enhanced long-term (weeks) function over those grown on materials made from larger crystallites.[11] Biomaterial composites composed of polymer and ceramic components can also increase the functional lifetime of implants and have also shown greater cytocompatibility and efficiency when ceramic grain sizes are less than 100 nm.[12] Incorporating nanoscale inorganic components in biocomposites has proven time and again to be a successful strategy for improving a material's modulus and its ability to interact effectively with the local cellular environment.

Many novel techniques have been developed recently to incorporate hydroxyapatite or similar calcium phosphate minerals into polymer matrices using in situ methods that mimic natural mineralization processes. Two of these methods are coprecipitation and ion diffusion, although there are others. Coprecipitation techniques to produce calcium phosphate/polymer composites are carried out in a liquid-phase reaction. In general, two solutions containing the calcium and phosphate precursors are prepared and then titrated together in the presence of a solvated polymer. In addition, this method can be carried out by the step-wise addition of calcium, phosphate, and polymer to a single reaction vessel. Coprecipitation has been extensively utilized in creating calcium phosphate composites with a wide range of natural and synthetic polymers, including polycaprolactone (PCL), poly(lactic-co-glycolic acid) (PLGA),[12] alginate,[13] collagen,[14] cellulose,[15] chitosan[16], and polymer blends (chitosan/dextran).[17]

Most relevant to our work, Enlow et al [18] used a variation of the coprecipitation technique to create composites comprising of a calcium phosphate mineral phase and a physically associating block copolymer gel. F127, a block copolymer, which forms thermoreversable gels, dissolved into a saturated calcium and phosphate solution at low temperature, can be heated to form a nanocomposite gel. Further modification of the coprecipitation technique has also been applied to concentrated solutions of anionic and zwitterionic pentablock copolymers with similar success.[19] More recently, coprecipitation has been used to incorporate Strontium-doped hydroxyapatite into chitosan/dextran hydrogels. These gels were biocompatible and able to promote osteogenesis in vivo.[17]

Ion diffusion techniques for composite formation provide another route for biomimetic design. Although this method is not utilized as often as the techniques mentioned previously, it has some inherent advantages. Unlike most coprecipitation formed composites, ion diffusion is used in gel systems; both chemically cross-linked and physically associated. In addition, this method tends only to be restricted by ion diffusion rates. Various experimental variables can be controlled to tune mineral content, phase, size, and morphology. Villacampa and Garcia-Ruiz[20] examined composites formed by ion diffusion of calcium into a phosphate-containing silica gel. When the initial pH of the gel was in the range of 10–12, pure hydroxyapatite was obtained, while reducing the pH altered the calcium phosphate mineral type grown in situ. In another study, using a silica gel, it was possible to examine the hydroxyapatite growth inhibition capabilities of various herbal extracts as treatments for musculoskeletal disorders.[21] Current induced ion diffusion techniques have also been further applied to polymer hydrogel systems, including gelatin[22] and polyacrylamide (PAAm).[23]

Herein, we report the synthesis of nanocrystalline calcium phosphate minerals in situ in gels of a commercially available block poly(ethylene oxide)-poly(propylene oxide)-poly(ethylene oxide) copolymer, F127. F127 has already been shown to be biocompatible and able to support osteogenesis when loaded with undifferentiated stem cells,[24] and to be degradable in vivo [25]. In contrast with Enlow et al[18], we use ion diffusion to directly synthesize the inorganic phase in the gel. Through manipulation of initial gel pH, we are able to obtain nano-sized domains of hydroxyapatite-like minerals in F127 gels.

While bone generally heals well on its own, severe damage from sources such as fractures or defects can greatly slow or prevent this process. Using scaffolds is one important method to aid recovery, as materials, such as hydroxyapatite, can be stored in the scaffold, and can have their mechanical properties tuned.[26] While many scaffolds will not have the stiffness of bone, around 10–20 GPa,[27] other softer tissues such as cartilage and muscle are still useful to mimic.[28,29] Of particular interest to this study gels with shear modulus between 15 and 30 KPa. Mesenchymal stem cells (MSC) preferentially differentiate into osteoblasts in environments with these moduli, making materials in this range of stiffness good candidates for bone regeneration.[30,31] Ciu et al showed that hydrogels with elastic moduli between 10 and 60 KPa aided in bone regeneration, while peak osteoblast differentiation of MSC is around 22 KPa.[29-31] It is our aim to design synthetic composites with these mechanical constraints in mind to gain a greater understanding of the mineralization process and as prototypes for biomaterials made with a novel in situ technique.

2 | MATERIALS AND METHODS

Characterization studies were used to determine the influence of pH on the mineralization process and compare that to those found in natural bone tissue. Small-amplitude oscillatory shear measurements allowed us to compare the impact of in situ formation versus conventional techniques on the mechanical properties of bioinspired composites.

Pluronic F127 hydrogels were formulated by the dissolution of 4.0 g of F127 (PEO_{99}-PPO_{65}-PEO_{99}; BASF; Germany) in 10.0 mL of 0.1 M phosphoric acid (H_3PO_4; Fisher Scientific; United States) at 0 °C in 20 mL scintillation vials. Unless otherwise noted, all solutions were prepared with nanopure water at a minimum resistance of 18 MΩ-cm. The initial pH of the phosphoric acid used was adjusted to either 7 or 11 by the addition of sodium hydroxide (NaOH; Mallinckrodt; United States) prior to F127 addition. Samples were vortexed to expedite complete solubilization of the polymer. After approximately 12 hours, the optically transparent solutions were moved to room temperature and allowed to gel.

A 2 mL aliquot of 1.0 M aqueous calcium chloride ($CaCl_2$; Acros Organics; Belgium) was pipetted onto the gel surface and allowed to diffuse into the hydrogel. An initial Ca:P molar ratio of 2:1 was chosen because it has been previously shown that this concentration ratio results in optimal mineralization and crystallinity for in situ composites.[32] Moreover, this ratio is similar to the physiological calcium-to-phosphate ratio found in blood plasma.

Mechanical characterization of the composite samples was carried out on an AR2000 stress-controlled rheometer (TA Instruments; United States) with 2° steel cone and plate geometry. Frequency sweep measurements were collected in the composites' linear viscoelastic region as determined by stress sweep measurements. All measurements were taken at 25 °C with a solvent trap to prevent evaporation. Conventionally prepared hydroxyapatite/F127 composites used for rheological comparison were created by incorporating 0–4 wt% hydroxyapatite (Sigma Aldrich; United States) in 25 wt % F127 hydrogels by rotor–stator homogenization (IKA UltraTurrax; Germany) at 18,000 rpm for 1 minute.

To isolate the mineral phase, composite gels were placed in 50 mL conical tubes and diluted with nanopure water to below the critical gelation concentration (1% w/v),[33] centrifuged using a Savant centrifugal evaporator, and aspirated. This washing procedure was repeated four times, after which the isolated solids were dried under air flow. Measurements taken after drying showed a total mineral content of the composite gels to be approximately 0.9%–1.1% for both the pH 7 and pH 11 composites.

Dry minerals were analyzed using powder X-ray diffraction (XRD) on a PANalytical X'Pert Material Research Diffractometer (PANalytical; The Netherlands). Dry mineral samples were milled with acetone in a mortar and pestle before being loaded onto a silicon zero-background plate for analysis. Mineral phases were identified using PANalytical X'Pert HighScore software, containing Powder Diffraction File search capabilities.

Calcium phosphate mineral particle size of the pH 11 composite was determined using a Coulter LS230 Laser Diffraction Particle Size Analyzer (Beckman Coulter; United States). Dried calcium phosphate crystals were suspended in acetone and sonicated prior to the analysis to disperse any agglomerated particles. Crystal size was further verified using a JEOL JSM 6320F field emission gun scanning electron microscope (FEG-SEM; JEOL; Japan). For this procedure, dried minerals were suspended in acetone and sonicated then passed through a 0.45 μm syringe filter to remove large particulates and aid in visualization. The samples were placed on aluminum sample mounts and coated with thin gold films before SEM examination.

3 | RESULTS AND DISCUSSION

Mineral formation was observed immediately once calcium was added to the gels. The calcium chloride solution became cloudy at the liquid–gel interface, and, over time, started to permeate into the gel. Mineralization in the hydrogel continued over the course of several days, preceding axially into the gel. After 2 days, the samples with pH 7 started to undergo a solid–solid transition. During this process, large crystallites with sizes on the order of millimeters became visible (Supplementary Information Figure S1, Figure S2). The second, large crystallite, phase grew over the course of 2 weeks in these samples until they visibly encompassed the entire domain. While there has been some research into the effect of pH on the mineralization of biologically relevant compounds, this area of the literature is still quite light. Phase differences at different pH values have been seen in other minerals, such as silicon[34] and calcification processes.[35] Calcium phosphate mineral phase varies in acidic vs. basic conditions and has been used as a pH sensing material.[36] Regardless, the pH effects of the phase of in situ mineralization is relatively unexplored.

XRD analysis of pH 7 composites identified the smaller larger particles as the mineral brushite ($CaHPO_4{\cdot}2H_2O$), a highly crystalline calcium phosphate. The scattering peaks (bottom spectrum) align well with commercially available brushite.[37] The smaller particles present in the pH 7 composites were identified as monetite ($CaHPO_4$), the anhydrous form of brushite. The inorganic phase formed at pH 11 differed significantly from the pH 7 mineral. When isolated and dried, the pH 11 mineral appeared as a fine white powder, similar to that of commercially available hydroxyapatite ($Ca_{10}(PO_4)_6(OH)_2$). Analysis of the powder XRD spectra reveals that the pH 11 mineral was calcium hydrogen phosphate hydrate ($Ca_8(HPO_4)_2(PO_4)_4(H_2O)_5$), a precursor to hydroxyapatite.[38] From the diffraction patterns shown in Figure 1, the calcium phosphate phase of the pH 11 material shows crystallographic peaks in *d*-spacing ranges similar to that of hydroxyapatite as well as peak-broadening characteristic[39] of nanoscale crystallites.

Samples formed at pH 7 exhibited a heterogeneous region of high mineral content at the surface of the composite. In this region, we observed another unique calcium phosphate phase. Small quantities of spherical particles were isolated from this heterogeneous boundary and determined by XRD analysis to consist of monetite ($CaHPO_4$) (spectra shown in Figure 1).[40] Micrograph images of the ca 250 μm monetite particles as well as the brushite and calcium hydrogen phosphate hydrate crystals confirm the results from the XRD analysis (Figure 2). Brushite shows a characteristic thin sheaf structure[37] while the monetite crystals are more porous, consisting of small thin intertwined strands.[40] It is possible that foaming of the polymer solution occurred during dissolution and solidified during gelation and acted as nucleation sites near the surface for this material.

Many calcium phosphate phases occur naturally and the behavior of calcium phosphates in the hydroxyapatite family is largely

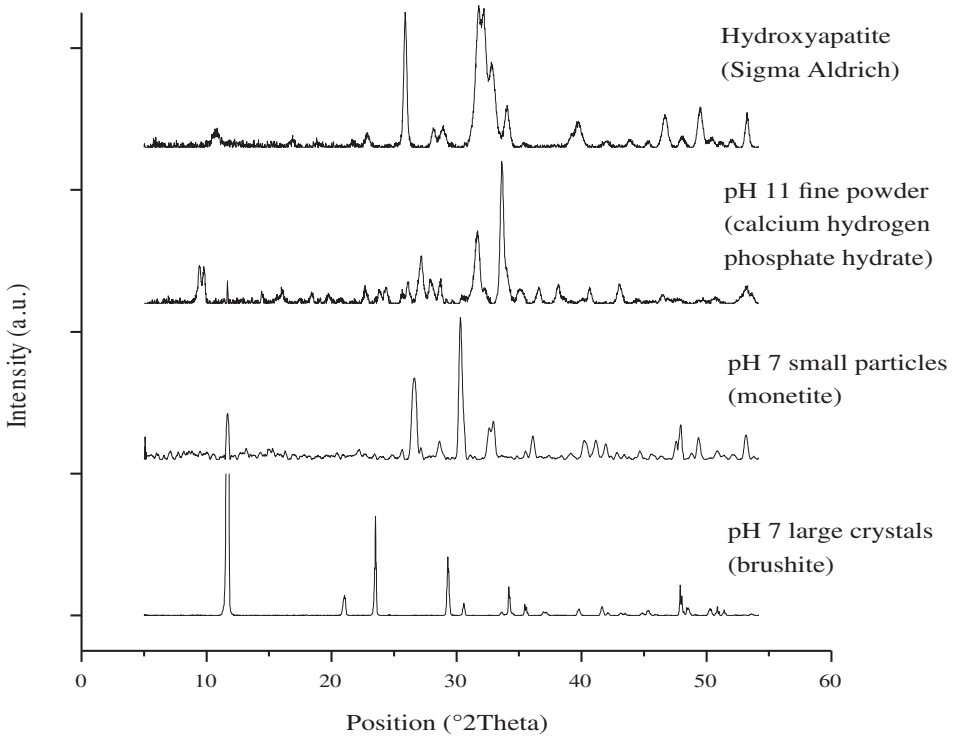

FIGURE 1 X-ray diffraction patterns of composite minerals and commercially available hydroxyapatite (HAp) taken on powders using a labscale PANalytical X'Pert Material Research Diffractometer. The intense brushite peak at $2\theta = 11.7^\circ$ has been truncated to prevent interference with the other spectra

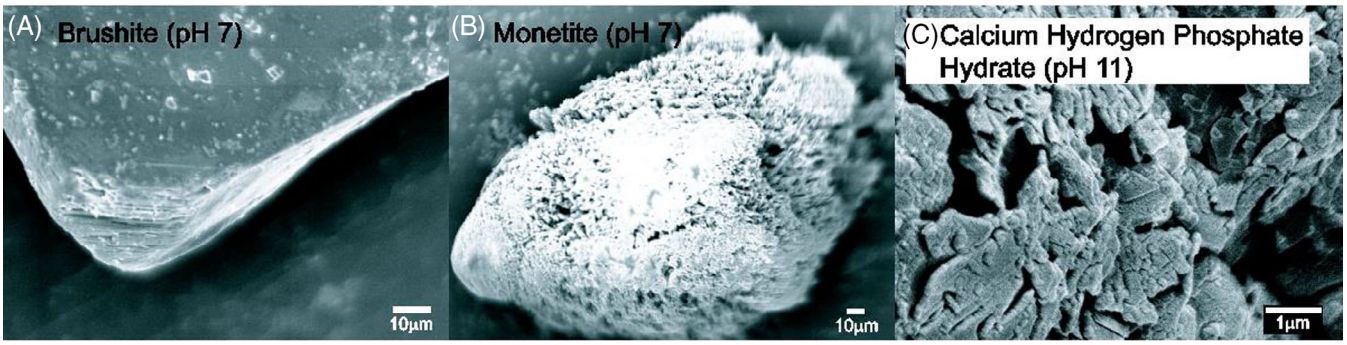

FIGURE 2 SEM micrographs of mineral phases recovered from the composite materials: A, highly crystalline brushite found throughout the pH 7 sample; B, porous monetite found near the interface of the pH 7 sample; and C, calcium hydrogen phosphate hydrate found in the pH 11 sample

dependent on the structure and composition of the mineral. Dissolution rate and bioactivity are dependent on such properties as follows: crystallinity, calcium/phosphate ratio, microstructure, surface area, and density.[41] Many calcium phosphates similar to hydroxyapatite in these regards are biologically relevant and are useful in the formation of biomaterials. As such, the mineral phase formed at pH 11 is a possible candidate for bone growth treatment. Calcium hydrogen phosphate hydrate has also been extensively studied and can be used as a precursor to form hydroxyapatite.[38]

The size and morphology of the inorganic phase are crucial to bioresorbability. Nanoscale structural features of biomaterials are also known to be crucial to cell functionality and adhesion for a variety of different cell types.[11,42] Figure 3 shows a particle-size distribution of the pH 11 mineral determined by laser diffraction. This distribution is approximately log-normal with the majority of particles between 50 and 300 nm in diameter. To act as a comparison, commercially available hydroxyapatite powder was also analyzed and found to exhibit a distribution very similar to the in situ formed mineral, although the commercial hydroxyapatite powder is slightly larger. Both the materials mineralized in the pH 11 gels and the commercially available hydroxyapatite are on the nano to sub-micron scale, with the peak in size around 100 nm. Hydroxyapatite's use in biological systems comes from attaching it to a scaffold that can be directed to a site of bone damage. By using these F127 gels, which are thermoreversable, as the scaffold, hydroxyapatite-like material can be synthesized directly into an injectable gel.

SEM images taken of the pH 11 mineral and commercial hydroxyapatite support the findings from light scattering. The SEM images, Figure 4A, agree with the laser diffraction experiments, showing that the calcium hydrogen phosphate hydrate particles are predominately

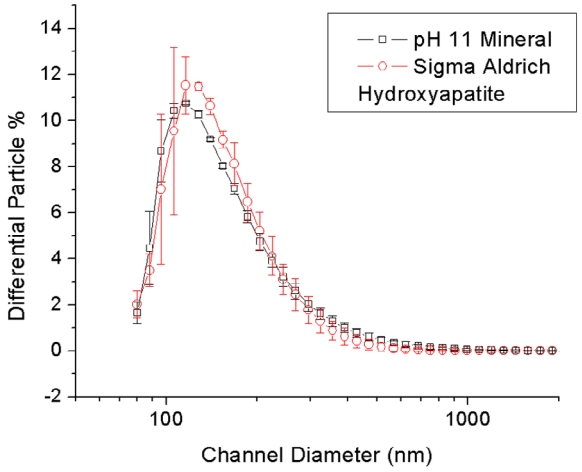

FIGURE 3 Coulter particle-size analyzer-size distribution for the mineral phase recovered from the composite synthesized in the hydrogel at pH 11 as compared to commercially available HAp

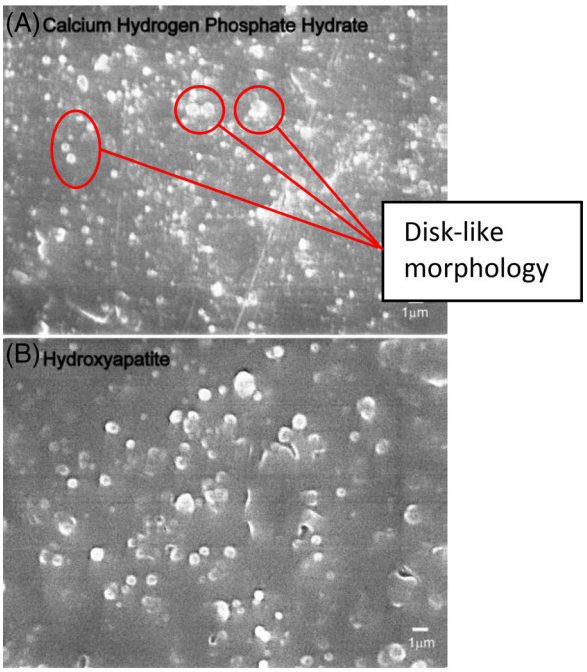

FIGURE 4 SEM images of A, pH 11 mineral recovered from the composite material and B, commercially available hydroxyapatite. Samples were passed through a 0.45 μm filter prior to imaging to remove large aggregates

in the size range of 50–300 nm. Commercially produced hydroxyapatite particles shown in Figure 4B are comparable in size. Furthermore, the particles of pH 11 mineral appear disc-like in morphology, which is similar to that of naturally occurring bone apatite, which forms ellipsoidal plates.

The SEM micrographs were analyzed to determine the particle-size distribution for both the pH 11 sample and the commercially available hydroxyapatite sample (Figure 5). While the sizes for both samples are quite close, the nanoparticles formed in situ are smaller

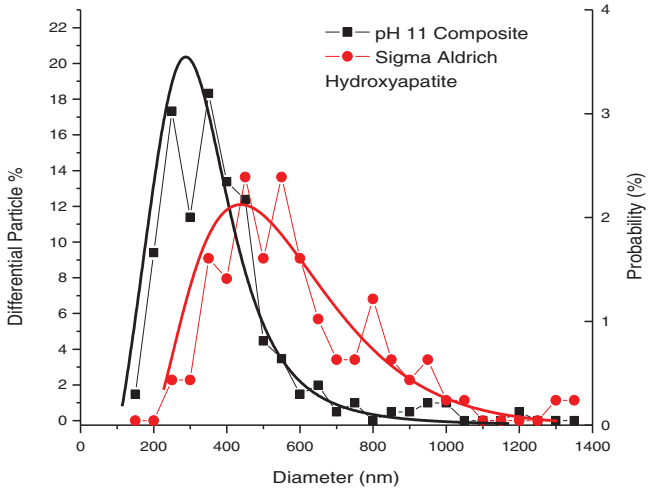

FIGURE 5 Particle-size distribution of the pH 11 sample and commercially available hydroxyapatite sample. The sizes were determined by analyzing SEM micrographs using ImageJ and best-fit probability distribution functions

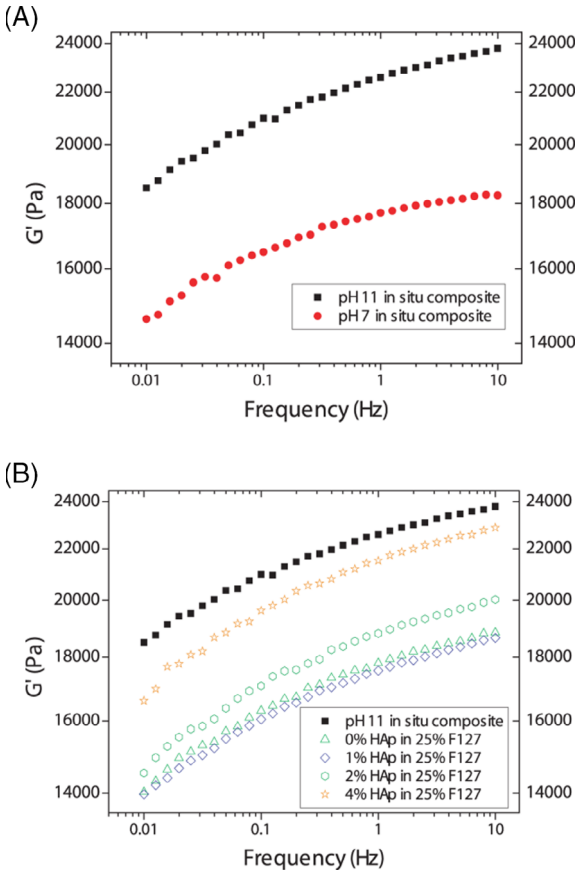

FIGURE 6 Storage moduli of A, in situ composites and B, conventionally prepared composites, measured under small-amplitude oscillatory shear on a stress-controlled rheometer. In situ composites contain approximately 1 wt% calcium phosphate mineral

and show a tighter size distribution. The size and distribution data were confirmed using DLS, which can be found in the supplementary information (Figure S3). As discussed in the background, nanoscopic

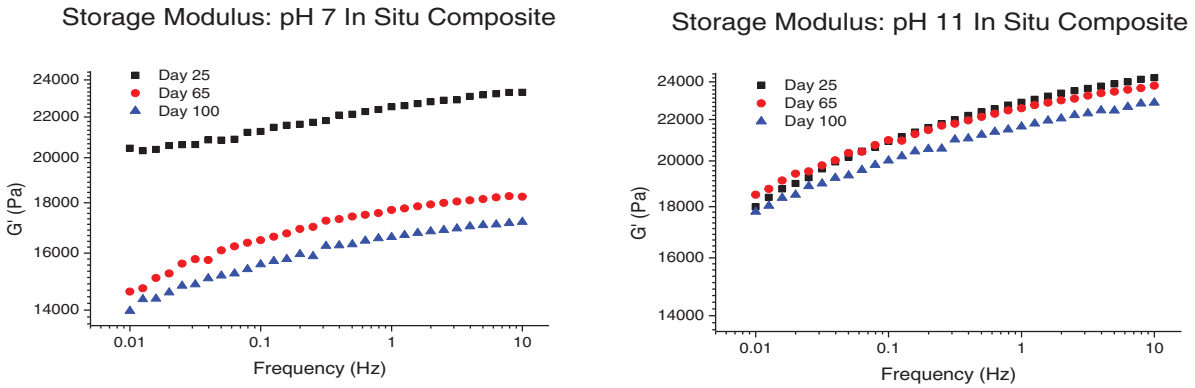

FIGURE 7 Stability of rheological properties of pH 7 (left) and pH 11 (right) samples over 100 days, showing a decrease in the storage modulus of the pH 7 composite as the sample ages

calcium phosphate shows a much higher biological resorption efficiency, which more closely resembles the effectiveness of actual hydroxyapatite.

Mechanical properties of biomaterials play a significant role in cellular phenotypic expression; and the development of mechanically robust composites containing inorganic calcium phosphate remains a significant challenge.[43] We investigated the elastic moduli of our in situ composites, taken in a region far from the interface where the gels are fairly homogenous, and compared these to conventionally prepared hydroxyapatite/F127 composites. Figure 6A shows that the elastic moduli for our samples are in the 15–25 kPa range. Although this is below the typical modulus of natural soft tissues such as articular cartilage, the results from Figure 6B show that the in situ composite formed at pH 11 exhibits a modulus greater than conventional prepared standards. The in situ composite shows the greatest modulus while containing only a fraction of the mineral content (approximately 1% total inorganic). The increase in modulus for the loaded samples is to be expected, as the mechanical properties of nanocomposites generally increase with increase in the filler content.[44] Composite theory, presented by Guth, also predicts that the shape of the filler particle accelerates the increase in the modulus.[45] Further modification and tuning of the modulus can likely be done by altering the concentration of the inorganic material, which can be easily done with the method described previously. This result suggests that the synthetic route utilized for composite formation may play an integral role in determining overall material properties.

Although the stiffness of these gels is lower than the modulus of bone and related tissues, such as tendons and cartilage, materials with similar mechanical properties have been used in successful bone remediation before. In cases of severe bone trauma, bone grafts are often the most effective method of treatment, although there can be numerous side effects and complications. Materials with shear moduli between 17 and 22 kPa applied to bone defect or damaged sites are among the most efficient at differentiating mesenchymal stem cells (MSC) into osteoblasts.[30,31,46] In addition to MSC responding to the stiffness of scaffold materials, gels loaded with nanominerals such as clays further increase the efficiency of MSC differentiation and new bone growth compared to empty gels with the same stiffness.[29] At pH 11, the stiffness of F127 gels loaded with nano-sized calcium hydrogen phosphate hydrate possess biologically relevant mechanical strengths. Furthermore, they are loaded with the material that can aid in bone growth.

Additional rheology was performed over a time period of 100 days to determine the consistency of the mechanical properties (Figure 7). The pH 7 and pH 11 samples behaved quite differently over this time period. In the pH 11 in situ composite, the strength of the sample remained nearly identical over the 100-day testing window. There is a slight drop in the strength over this period, but it remains in the same order of magnitude. The pH 7 sample, however, showed a much higher depreciation in strength by 65 days after calcium addition. This is likely due to some of the larger crystallites precipitating out of the mixture and settling toward the bottom of the gel, where the pH 11 sample contains nano-sized crystallites that are well incorporated into the gel structure.

4 | CONCLUSIONS

Calcium phosphate crystals were synthesized in situ in a physically associating block copolymer gel using a simple chemical synthesis technique and readily available components. The initial pH of hydrogels plays a vital role in determining crystal phase, size, and morphology. These are primary characteristics in determining the effectiveness of a biomaterial in vivo. Gels at an initial pH of 7 induce the growth of macroscopic crystals of brushite, whereas calcium hydrogen phosphate hydrate particles, with diameters in the range of 50–300 nm, form in composites with initial pH of 11. The in situ method of composite synthesis shows improved mechanical strength over conventionally prepared polymer/calcium phosphate composites, even with less total inorganic content. This mechanical strength is in the ideal range for the differentiation of MSC into osteoblasts and promoting new bone growth.

We recognize the need for further optimization and refinement before similar materials could be explored for in vivo applications.

Because the F127 matrix is thermo-reversible, one potential application would be to use similar materials to aid in seeding calcium phosphate nanoparticles and cells into more robust porous scaffolds. Similar uses of F127 gels as cell seeding agents have been discussed in the literature.[47] Another possible use of this system is as an injectable hydrogel, which allows for less invasive targeted implanting, and could be a desirable alternative to grafting surgeries. The high pH required to obtain nanoscale calcium phosphate domains is also problematic in terms of biological applications; we are currently exploring other routes to mediate this effect. Nevertheless, our work demonstrates the utility of this in situ synthetic approach to creating new nanocomposite biomaterials.

ACKNOWLEDGEMENTS

Support for DMG was provided by the NSF IGERT program in Nanotechnology Innovation (DGE-0504485) and an NIH-sponsored Chemistry-Biology Interface Training Grant (National Research Service Award T32 GM08515), and support for MAK was provided by an NSF NRT award, DGE-1922639. The research utilized central facilities of the NSF-funded IGERT in Cellular Engineering (DGE-0654128) and the NSF-funded Center for Hierarchical Manufacturing (CMMI-0531171). The authors thank BASF for the donation of Pluronic F127. Neither the sponsoring agencies nor BASF had any role in the study design; in the collection, analysis, and interpretation of data; in the writing of the report; and in the decision to submit the paper for publication.

ORCID

Surita R. Bhatia https://orcid.org/0000-0002-5950-193X

REFERENCES

1. Olszta MJ, Cheng X, Jee SS, et al. Bone structure and formation: a new perspective. *Mater Sci Eng R*. 2007;58:77-116.
2. Nightingale JP, Lewis D. Pole figures of the orientation of apatite in bones. *Nature*. 1971;232(5309):334-335.
3. Wang Y, Azaïs T, Robin M, et al. The predominant role of collagen in the nucleation, growth, structure and orientation of bone apatite. *Nat Mater*. 2012;11(8):724-733.
4. Mauffrey C, Madsen M, Bowles RJ, Seligson D. Bone graft harvest site options in orthopaedic trauma: a prospective in vivo quantification study. *Injury*. 2012;43(3):323-326.
5. Shikinami Y, Okuno M. Bioresorbable devices made of forged composites of hydroxyapatite (HA) particles and poly-L-lactide (PLLA). Part I: basic characteristics. *Biomaterials*. 1999;20:859-877.
6. Sun T-W, Zhu Y-J, Chen F. Hydroxyapatite nanowire/collagen elastic porous nanocomposite and its enhanced performance in bone defect repair. *RSC Adv*. 2018;8(46):26218-26229.
7. Murugan R, Ramakrishna S. Development of nanocomposites for bone grafting. *Compos Sci Technol*. 2005;65:2385-2406.
8. Pan Y, Xiong D, Gao F. Viscoelastic behavior of nano-hydroxyapatite reinforced poly(vinyl alcohol) gel biocomposites as an articular cartilage. *J Mater Sci Mater Med*. 2008;19:1963-1969.
9. Li Y, Zhang Y, Shi F, Tao L, Wei Y, Wang X. Modulus-regulated 3D-cell proliferation in an injectable self-healing hydrogel. *Colloids Surf B Biointerfaces*. 2017;149:168-173.
10. Murugan R, Ramakrishna S. Aqueous mediated synthesis of bioresorbable nanocrystalline hydroxyapatite. *J Cryst Growth*. 2005;274:209-213.
11. Webster TJ, Ergun C, Doremus RH, Siegel RW, Bizios R. Enhanced functions of osteoblasts on nanophase ceramics. *Biomaterials*. 2000;21:1803-1810.
12. Huang J, Xia X, Zou Q, et al. The long-term behaviors and differences in bone reconstruction of three polymer-based scaffolds with different degradability. *J Mater Chem B*. 2019;7(48):7690-7703.
13. Salimi E. In-situ synthesis of a novel Bioresorbable sodium alginate/hydroxyapatite–calcium pyrophosphate nanocomposite as bone replacement. *J Inorg Organomet Polym Mater*. 2019;30:1769-1775.
14. Lin X, Li X, Fan H, Wen X, Lu J, Zhang X. In situ synthesis of bone-like apatite/collagen nano-composite at low temperature. *Mater Lett*. 2004;58:3569-3572.
15. Zhang J, Iwasa M, Jiang D. Size-controlled hydroxyapatite nanoparticles as self-organized organic-inorganic composite materials. *Adv Sci Technol*. 2006;53:32-37.
16. Nikpour MR, Rabiee SM, Jahanshahi M. Synthesis and characterization of hydroxyapatite/chitosan nanocomposite materials for medical engineering applications. *Compos Part B Eng*. 2012;43(4):1881-1886.
17. Ding X, Li X, Li C, et al. Chitosan/dextran hydrogel constructs containing strontium-doped hydroxyapatite with enhanced osteogenic potential in rat cranium. *ACS Biomater Sci Eng*. 2019;5(9):4574-4586.
18. Enlow D, Rawal A, Kanapathipillai M, et al. Synthesis and characterization of self-assembled block copolymer templated calcium phosphate nanocomposite gels. *J Mater Chem*. 2007;17:1570-1578.
19. Kanapathipillai M, Yusufoglu Y, Rawal A, et al. Synthesis and characterization of ionic block copolymer templated calcium phosphate nanocomposites. *Chem Mater*. 2008;20:5922-5932.
20. Villacampa AI, Garcia-Ruiz JM. Synthesis of a new hydroxyapatite-silica composite material. *J Cryst Growth*. 2000;211:111-115.
21. Parekh B, Joshi M, Vaidya A. Characterization and inhibitive study of gel-grown hydroxyapatite crystals at physiological temperature. *J Cryst Growth*. 2008;310:1749-1753.
22. Heinemann C, Heinemann S, Kruppke B, et al. Electric field-assisted formation of organically modified hydroxyapatite (ormoHAP) spheres in carboxymethylated gelatin gels. *Acta Biomater*. 2016;44:135-143.
23. Li Z, Wen T, Su Y, Wei X, He C, Wang D. Hollow hydroxyapatite spheres fabrication with three-dimensional hydrogel template. *CrstEngComm*. 2014;16(20):4202-4209.
24. Chen W-J, Huang J-W, Niu C-C, et al. Use of fluorescence labeled mesenchymal stem cells in pluronic F127 and porous hydroxyapatite as a bone substitute for posterolateral spinal fusion. *J Orthop Res*. 2009;27(12):1631-1636.
25. Zhang J, Zhou J, Huang X, Wang L, Liu G, Cheng J. In situ preparation of hierarchically porous β-tricalcium phosphate bioceramic scaffolds by the sol-gel method combined with F127. *Ceram Int*. 2020;46(5):6396-6405.
26. Pacelli S, Basu S, Whitlow J, et al. Strategies to develop endogenous stem cell-recruiting bioactive materials for tissue repair and regeneration. *Adv Drug Deliv Rev*. 2017;120:50-70.
27. Rho JY, Ashman RB, Turner CH. Young's modulus of trabecular and cortical bone material: ultrasonic and microtensile measurements. *J Biomech*. 1993;26(2):111-119.
28. Robinson DL, Kersh ME, Walsh NC, Ackland DC, de Steiger RN, Pandy MG. Mechanical properties of normal and osteoarthritic human articular cartilage. *J Mech Behav Biomed Mater*. 2016;61:96-109.
29. Cui Z-K, Kim S, Baljon JJ, Wu BM, Aghaloo T, Lee M. Microporous methacrylated glycol chitosan-montmorillonite nanocomposite hydrogel for bone tissue engineering. *Nat Commun*. 2019;10(1):3523.
30. Wen JH, Vincent LG, Fuhrmann A, et al. Interplay of matrix stiffness and protein tethering in stem cell differentiation. *Nat Mater*. 2014;13(10):979-987.

31. Huebsch N, Arany PR, Mao AS, et al. Harnessing traction-mediated manipulation of the cell/matrix interface to control stem-cell fate. *Nat Mater*. 2010;9(6):518-526.
32. Das P, Akkus O, Azad A-M. Optimization of the mineral content in polymeric gels: the effect of calcium to phosphate molar ratio. *J Cryst Growth*. 2005;280:587-593.
33. Alexandridis P, Holzwarth JF, Hatton TA. Micellization of poly(ethylene oxide)-poly(propylene oxide)-poly(ethylene oxide) triblock copolymers in aqueous solutions: thermodynamics of copolymer association. *Macromolecules*. 1994;27:2414-2425.
34. Hervé V, Derr J, Douady S, Quinet M, Moisan L, Lopez PJ. Multiparametric analyses reveal the pH-dependence of silicon biomineralization in diatoms. *PLoS One*. 2012;7(10):e46722.
35. Goffredo S, Prada F, Caroselli E, et al. Biomineralization control related to population density under ocean acidification. *Nat Climate Change*. 2014;4(7):593-597.
36. Dias CI, Mano JF, Alves NM. pH-responsive biomineralization onto chitosan grafted biodegradable substrates. *J Mater Chem*. 2008;18 (21):2493-2499.
37. Arifuzzaman SM, Rohani S. Experimental study of brushite precipitation. *J Cryst Growth*. 2004;267(3):624-634.
38. Francis MD, Webb NC. Hydroxyapatite formation from a hydrated calcium monohydrogen phosphate precursor. *Calcif Tissue Res*. 1970; 6(1):335-342.
39. Venkateswarlu K, Chandra Bose A, Rameshbabu N. X-ray peak broadening studies of nanocrystalline hydroxyapatite by Williamson–hall analysis. *Phys B Condens Matter*. 2010;405(20): 4256-4261.
40. Prado Da Silva MH, Lima JHC, Soares GA, et al. Transformation of monetite to hydroxyapatite in bioactive coatings on titanium. *Surf Coat Technol*. 2001;137(2):270-276.
41. Radin SR, Ducheyne P. The effect of calcium phosphate ceramic composition and structure on in vitro behavior. II. Precipitation. *J Biomed Mater Res*. 1993;27(1):35-45.
42. Doiron AL, Clark B, Rinker KD. Endothelial nanoparticle binding kinetics are matrix and size dependent. *Biotechnol Bioeng*. 2011;108(12):2988-2998.
43. Liu H, Webster TJ. Mechanical properties of dispersed ceramic nanoparticles in polymer composites for orthopedic applications. *Int J Nanomedicine*. 2010;5:299-313.
44. Wu Y-P, Jia Q-X, Yu D-S, Zhang L-Q. Modeling Young's modulus of rubber–clay nanocomposites using composite theories. *Polym Test*. 2004;23(8):903-909.
45. Guth E. Theory of filler reinforcement. *J Appl Phys*. 1945;16(1):20-25.
46. Chaudhuri O, Gu L, Klumpers D, et al. Hydrogels with tunable stress relaxation regulate stem cell fate and activity. *Nat Mater*. 2016;15(3):326-334.
47. Khattak SF, Bhatia SR, Roberts SC. Pluronic F127 as a cell encapsulation material: utilization of membrane-stabilizing agents. *Tissue Eng*. 2005;11(5–6):974-983.

SUPPORTING INFORMATION

Additional supporting information may be found online in the Supporting Information section at the end of this article.

How to cite this article: Griffin DM, Kennedy MA, Bhatia SR. Calcium phosphate nanocomposites via in situ mineralization in block copolymer hydrogels. *Polym Adv Technol*. 2021;32: 1372–1379. https://doi.org/10.1002/pat.5183